

is possible in Figs. 1, 2, and 3. The observed durations of the solar flares are also indicated as well as the times of commencement of the radio fadeouts.

In addition to complete shielding by 12-cm Pb, the meter at Climax was under a rectangular iron shield 4 ft. long, 1 ft. wide, and 16.5 cm thick. The absorption mean free path for nucleons of medium energy in iron is approximately  $240 \text{ g cm}^{-2}$ . Taking the dimensions of the shield into account and figuring the zenith angle distribution for a radiation exponentially absorbed with an absorption coefficient of about  $145 \text{ g cm}^{-2}$ , it is estimated that the increase at Climax on November 19, 1949, would have been 15 percent greater without the iron shield. Thus it is estimated that the maximum of the increase on November 19 at Climax would have been about 207 percent without the iron shield, instead of the uncorrected 180 percent as shown in Figs. 3 and 4. This correction also results in a factor of 4.8 for the ratio of the percentage increase at Climax on November 19 relative to that at Cheltenham, instead of 4.2 as is indicated in Fig. 4.

Since the total ionization at Climax (under 12-cm Pb) is about 2.5 times that at Cheltenham, and since the percentage increase on November 19, 1949, was about 4.8 times that at Cheltenham, the actual magnitude of the increase on that date at Climax was about 12 times greater than at Cheltenham. Since the difference in the atmospheric layer is equivalent to  $340 \text{ g cm}^{-2}$ , the radiation responsible for the increase during the flare has an absorption coefficient of about  $137 \text{ g cm}^{-2}$ . This is just about the rate at which the nucleonic component, responsible for star production, increases with altitude.<sup>5</sup> The increase in total ionization under 12-cm Pb by a factor of 2.5 from Cheltenham to Climax is mainly due to mesons. It is thus evident that the magnitude of the

<sup>5</sup> J. J. Lord and Marcel Schein, *Phys. Rev.* **75**, 1956 (1949).

flare effect increases too rapidly with altitude to be ascribed to ordinary mesons. The latitude effect in chambers under 12-cm Pb, due principally to mesons, is small, whereas the flare effect exhibits a strong dependence on latitude (being zero at the equator). This also indicates that ordinary mesons contribute negligibly to the flare effect.

The results of Conversi<sup>6</sup> and those of Simpson<sup>7</sup> on the latitude variation of the proton and neutron intensity suggested that the cross section for nucleon production relative to that for meson production decreases rapidly with increasing energy of primary particles. This is in accord with the conclusion that the increase in intensity during the solar flare of November 19, 1949, was due principally to the nucleonic component or to local radiations originating from it, and not to ordinary mesons.

At Climax, under 12-cm Pb, probably not more than about 10 percent of the total ionization is normally due to local radiation originating from the nucleonic component. If we assume that this radiation is produced entirely by particles in the same band of energy as those responsible for the increase of 207 percent in ionization on November 19, 1949, then the number of primary particles, reaching there per unit time, in that band of energy, must have increased to at least 20 times the normal value.

Three sets of triple coincidence counters and one set of fourfold coincidence counters, located above the meter at Climax and arranged to record air showers, were in continuous operation during the period of the increase in ionization on November 19, 1949. There was no evidence of any significant increase in the rate of air showers during this period.

<sup>6</sup> Marcello Conversi, *Phys. Rev.* **76**, 444 (1949).

<sup>7</sup> J. A. Simpson, Jr., *Phys. Rev.* **76**, 569 (1949).

## Ratio of Cross Sections for Electron Capture and Electron Loss by Proton Beams in Metals

THEODORE HALL

*Institute for Nuclear Studies, University of Chicago, Chicago, Illinois*

(Received March 2, 1950)

Measurements have been made of the ratio of the charged to the neutral component (protons to hydrogen atoms) in hydrogen ion beams of energies between 20 and 400 kv, passing through the metallic media beryllium, aluminum, silver, and gold. The data show that this ratio is the same, within the accuracy of the experiment, for the three lighter elements, but is slightly less in gold above 100 kv. The curves depicting this ratio as a function of ion speed cannot be fitted by a power law over the entire energy range, but the high energy end of the data can be fitted fairly well in this way. At 350 kv, the slopes correspond to a dependence on ion speed  $v$  of the form  $v^9$  in the case of the lighter elements, and  $v^7$  in the case of gold.

The cross sections for electron capture and electron loss are found to be equal at an ion energy of 26 kv. The ion then has a speed 0.95 times that of the hydrogen orbital electron ( $e^2/\hbar$ ).

### I. INTRODUCTION

FOR several reasons there is interest in the capture and loss of electrons by light ions as they pass through matter: the phenomena themselves are funda-

mental atomic processes; the charge of these ions influences their slowing down; and furthermore, in the case of the light ions it is possible to test present ideas about electron capture and loss which apply to the

stopping of fission fragments, where charge of the fragment plays a major role.

An incomplete listing of previous work on this subject is given.<sup>1-15</sup> References 1 to 4 deal with experimental work on hydrogen canal rays, 5 to 9 with experimental work on alpha-rays, 10 and 11 with the classical theory of electron capture, 12 and 13 with the quantum-mechanical theory of capture, and 14 and 15 with general surveys on the field. The article by Bohr,<sup>15</sup> offers simple ideas for handling the difficult problem of electron capture under a wide range of conditions, and the present data will be considered largely in the light of these ideas.

In studying the average charge of fast ions, these specific questions are of the greatest interest: how does the state of charge depend on the speed of the ion, how does it depend on the stopping medium, and at

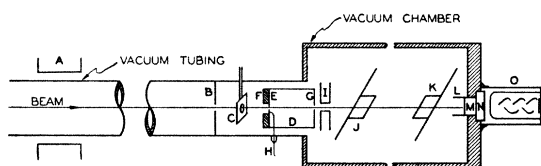


FIG. 1. Apparatus, schematic.

what ion speed is it equally likely for a given electron orbit to be filled or unfilled? An experimental answer to these questions is most instructive in the case of hydrogen ions, for which the theory is simplest. It is also desirable to investigate light ions of speeds near the speed  $v_0 = e^2/h$ , because capture and loss cross sections are then nearly equal. Data for hydrogen ions of such speeds has not previously been available, since the experimental studies cited use either alpha-rays from radioactive sources, or low speed hydrogen canal rays.

The present work is a study of hydrogen ions, of speeds between  $v_0$  and  $4v_0$  (energies between 20 and 400 kv), provided by the University of Chicago Cockcroft-Walton accelerator.<sup>16</sup> Thin metallic foils were placed in the path of the ion beam, and the emerging beam, whose energy was accurately known, was an-

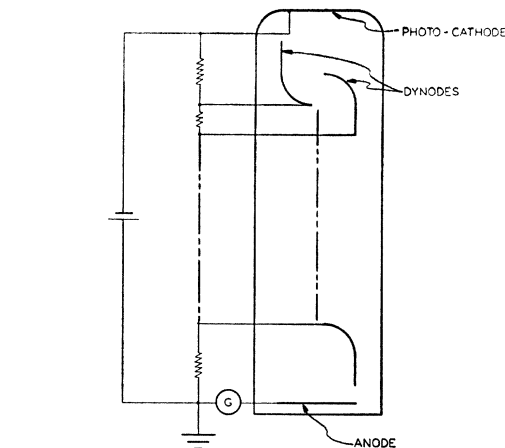


FIG. 2. Photo-multiplier circuit.

alyzed into neutral and charged components. In order to study the dependence of the charge state upon the atomic number of the foil material, foils of beryllium, aluminum, silver, and gold were used. Since the beam quickly comes to a state of charge equilibrium in the foils, the data do not give information about the absolute size of the cross sections for electron capture and loss. The results reported here are in the form of ratios of the loss to the capture cross section, as a function of hydrogen ion speed and stopping medium.

## II. EXPERIMENTAL ARRANGEMENT

The apparatus is shown schematically in Fig. 1. Everything shown there is kept at high vacuum except the photo-multiplier tube, O. The energy of the beam is obtained by measuring the current through a resistor stack placed between ground potential and the high voltage end of the accelerator. As the beam leaves the accelerating tube, it is analyzed magnetically at A; the selected component, either  $H^+$  or  $H_2^+$ , then travels down a 50-in. tube to B, where a 3/16-in. hole improves its definition. It then strikes the foil under study, mounted over a circular hole in a thin brass frame, C, which can be moved into or out of the beam by means of a Wilson seal. After emerging from the foil, the beam has the charge composition characteristic of the foil material and the energy of the emerging beam. Beam particles which have not undergone excessive Rutherford scattering can then pass through a 6-in. collimating tube, D, which has collimating holes (No. 70 drill size) in its brass end plates, E and G. After collimation the beam travels 20 in. to a potassium iodide (thallium enriched) crystal, M; light from the crystal leaves the vacuum chamber through a glass window, N, and a galvanometer is used to record the anode current produced by this light in the adjacent photo-multiplier tube, O (RCA Type 5819). Two electrodes at I, directly after collimation, can be used to apply a strong electric field to the beam. With this field turned off the multiplier current is proportional to the strength of the en-

<sup>1</sup> J. Konigsberger and J. Kutchewsky, *Ann. d. Physik* **37**, 195 (1912).

<sup>2</sup> E. Ruchardt, *Ann. d. Physik* **71**, 377 (1923).

<sup>3</sup> A. Ruttenuer, *Zeits. f. Physik* **4**, 267 (1921).

<sup>4</sup> H. Bartels, *Ann. d. Physik* **6**, 957 (1930).

<sup>5</sup> E. Rutherford, *Phil. Mag.* **47**, 277 (1924).

<sup>6</sup> P. Kapitza, *Proc. Roy. Soc.* **106**, 602 (1924).

<sup>7</sup> G. H. Henderson, *Proc. Roy. Soc.* **109**, 157 (1925).

<sup>8</sup> G. H. Briggs, *Proc. Roy. Soc.* **114**, 241 (1927).

<sup>9</sup> C. Gerthsen, *Physik. Zeits.* **31**, 948 (1930).

<sup>10</sup> R. H. Fowler, *Phil. Mag.* **47**, 416 (1924).

<sup>11</sup> L. H. Thomas, *Proc. Roy. Soc.* **114**, 561 (1927).

<sup>12</sup> J. R. Oppenheimer, *Phys. Rev.* **31**, 349 (1928).

<sup>13</sup> H. C. Brinkman and H. A. Kramers, *Proc. Akad. Amsterdam* **33**, 973 (1930).

<sup>14</sup> J. Knipp and E. Teller, *Phys. Rev.* **59**, 659 (1941).

<sup>15</sup> N. Bohr, *The Penetration of Atomic Particles through Matter* (Kgl. Danske Vid. Sels., 1948). This book can be obtained in America from Stechert and Company, New York.

<sup>16</sup> Allison, del Rosario, Hinton, and Wilcox, *Phys. Rev.* **71**, 139(A) (1947).

tire beam; with the field on it is proportional to the strength of the neutral component alone.<sup>17</sup> The difference between the two readings of course corresponds to the charged component. The data thus yield the ratio of the charged to the neutral component of the beam.

As to the further details shown in Fig. 1, *J* is a brass shutter which can be rotated through a Wilson seal to cut the beam off completely from the crystal, so that the background current of the multiplier tube can be corrected for. *K* is a similar shutter which is made of glass and swings into place directly in front of the crystal; its function is discussed below. *L* is a brass tube which serves to mount the crystal and also to shield it from stray radiation. *F* is a plastic cap which covers most of the insulated collimating plate *E*, leaving only a few square millimeters exposed to the beam, and *H* is a lead going from *E* to the outside through a Kovar seal. Since neutral and total beams are not measured simultaneously, correction is made for beam fluctuations by normalizing all multiplier readings to simultaneous readings of the current delivered through *H*. The collection of secondary electrons from the foil is avoided here by maintaining the plate *E* at a negative potential of approximately 200 v. The current to *E* ranges from 0.1 to 5  $\mu$ a and is read with a d.c. amplifier or directly by galvanometer. One further feature should be mentioned: the photo-multiplier background is very sensitive to extraneous light and also to slight

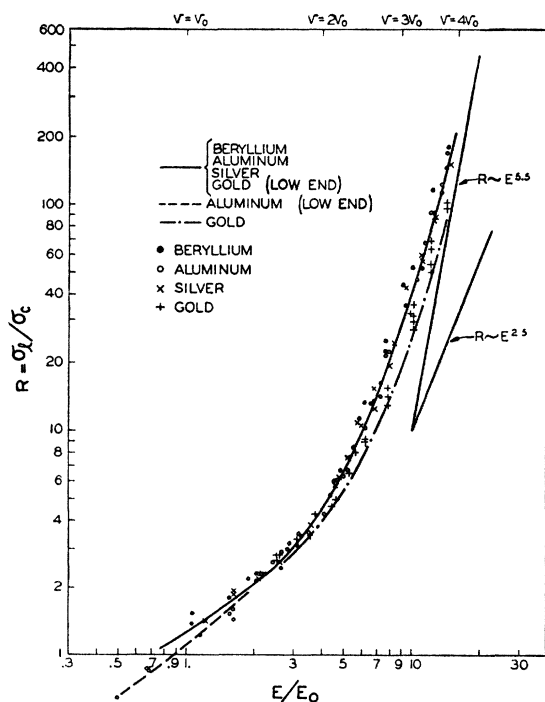


FIG. 3. Ratio of loss to capture cross section  $\sigma_l/\sigma_c$  as a function of ion energy  $E$ . At energy  $E_0$  the ion speed  $v = v_0 = e^2/\hbar$ .  $E_0 = 24.8$  kev.

<sup>17</sup> The crystal response is the same to neutral and to charged particles because an ion changes its state of charge many times as soon as it enters the crystal.

mechanical vibration. The background was kept low by fitting a Bakelite cylinder snugly onto the tube base and then sealing the Bakelite to the vacuum chamber with apiezon clay, an arrangement which is entirely opaque and avoids rigid mechanical coupling. The tube was supported with rubber-cushioned clamps.

The photo-multiplier circuit is shown in Fig. 2. Proper potentials between the tube electrodes are maintained by a regulated voltage supply feeding a set of bleeder resistances as shown. The first multiplication surface is the photo-cathode, which is a coating applied directly to the glass wall of the tube. The galvanometer is placed in the circuit as illustrated, between ground and anode.<sup>18</sup> The anode current never exceeded 15  $\mu$ a during the measurements, while the tube is rated for a maximum of  $\frac{3}{4}$   $\mu$ a, so that linearity is assured.

At ion speeds where the total beam was of the order of 10 times the neutral component, the two were compared by shunting the galvanometer, in order to keep its deflection fairly constant. At higher ion speeds, the ratio of the total to the neutral component was found to be of the order of 100:1. Strongly shunting the galvanometer for these measurements was awkward for technical reasons, so an alternative procedure was adopted. A careful calibration curve was run for the multiplier tube, plotting current gain *vs.* tube voltage, and the very unequal total and neutral beams were then observed using different tube voltages. The calibration curve was run by admitting light into the vacuum chamber near point *I* (Fig. 1).

Calibrating the multiplier provides notable flexibility. Since the current gain of the tube changes by a factor of about  $10^5$  as tube voltage goes from 400 to 1400 v, the ratio of largest and smallest beams easily comparable by this method is of the order of one million to one.

### III. THIN FOIL TECHNIQUE

The foils had to meet stringent requirements. In the first place, due to the severe collimation, Rutherford scattering in the foils eliminated most of the beam, so that any pinholes transmitting intense unscattered pencils would be intolerable. Second, the foils must have known uniform thickness so that the energy of the emergent beam may be well established.

Adequate foils were produced by covering the foil frames first with a very thin layer of Nylon or zapon (approximately 0.005 mg/cm<sup>2</sup>) and then evaporating the metal onto this backing.<sup>19</sup> In use the beam is directed into the side with the backing, of course.

<sup>18</sup> In this arrangement, the voltage drop across the galvanometer subtracts from the voltage between the last dynode and the collecting electrode, so that the multiplier gain is slightly reduced as current increases. This effect was small enough to require no correction.

<sup>19</sup> We are grateful to Dr. Hugh Bradner of the University of California for supplying us with beryllium foil produced by a different evaporation technique. We used these foils before learning to make our own, and obtained the same results with both sets

Foil thickness was measured by exposing half of an interferometer mirror placed adjacent to the foil frames during evaporation, and measuring displacement of the interference fringes. The energy loss was then calculated on the basis of the recent work in our laboratory on the slowing down of hydrogen ions of the same speeds in the same media.<sup>20</sup> No allowance was made for the Nylon or zapon backing in calculating this loss, since most of the backing undoubtedly burned off under the beam, leaving a negligible carbon deposit.

The foils ranged from  $\frac{1}{4}$  to  $\frac{1}{2}$  in. in diameter, and from 0.01 to 0.3 mg/cm<sup>2</sup> in thickness. The ions lost between 5 and 50 kv in crossing them. It was a pleasant surprise that these foils stood up for hours without showing any damage under beams as strong as 3  $\mu$ a concentrated on 0.2 cm<sup>2</sup>. Only in the case of the very thin gold foils, 0.02 mg/cm<sup>2</sup>, did such beams annihilate the foil, and this was presumably because the foil was so thin that it could not hold together once the backing was destroyed.

#### IV. EXPERIMENTAL PROCEDURE

During the actual runs the procedure was as follows. The ion beam was set to a particular energy and the foil placed in its path. Then readings of the multiplier current were taken, with the deflecting field first turned off and then turned on. The monitor current at point *E* (Fig. 1) was taken simultaneously with each reading. The field-off-field-on pairs were repeated two or more times to check the consistency of the readings and to reduce random errors. Then the shutter was placed in the way of the beam; background currents were observed; the accelerator was adjusted to a different beam energy and the cycle repeated. Since the beam area was much less than the foil area, the foil position could be changed several times in the course of a run, and foil uniformity was checked further by noting the stability of the multiplier current while moving the foil. Generally the beam could be passed over almost the entire foil with current fluctuations of only a few percent, and the results showed no dependence on foil position. Consistency was tested further by running the early and late points of a run at the same ion energies; results of this test were satisfactory except in the case of some of the gold runs, and the significance of this point is discussed below.

For the higher energy points it was feared that the very thin foils might not be thick enough to establish charge equilibrium. (Capture and loss cross sections decrease as energy increases, for ion speeds above  $v_0$ .) On the other hand, several reasons made very thin foils desirable for the lower energy points: for these points, straggling in the thicker foils and experimental uncertainty in the rate of energy loss lead to a serious percentage uncertainty in the final beam energy, and strong Rutherford scattering and weaker crystal

response create a sensitivity problem. Consequently, for each element two or more foils of different thicknesses were used. By overlapping data taken with these foils, it was guaranteed that charge equilibrium was established in the foils.

It may be assumed that charge equilibrium was established in all of the observations, since no dependence on foil thickness was ever noted. Such dependence could probably have been observed, had the study of the very thin gold foil been extended to the highest energies available. Detection of this dependence would have provided approximate absolute values for the capture and loss cross sections. In the present data, the thin gold foil (0.028 mg/cm<sup>2</sup>) was studied up to the ion energy of 132 kv (ion speed 2.3  $v_0$ ); the fact that charge equilibrium was still established means that the foil had a thickness of at least one mean free path at this energy, corresponding to a cross section of at least  $10^{-17}$  cm<sup>2</sup>. As is indicated in Section V, this figure refers strictly to the sum of capture and loss cross sections. Since the loss cross section is much the larger at this speed, it essentially provides a lower limit to the loss cross section.

#### V. EMPIRICAL MATHEMATICAL DESCRIPTION OF CAPTURE AND LOSS

To interpret the data, we need an elementary description of the beam's fate in the foil. Let  $N$  be the number of atoms per square centimeter in the foil,  $x$  the number of atoms per square centimeter from the front face of the foil to a variable position in the foil,  $\sigma_c$  and  $\sigma_l$  the cross sections per atom for electron capture and loss by the beam particles, and  $f_1(x)$  and  $f_0(x)$  the fractions of the beam which are singly charged and uncharged at  $x$ . The quantity measured in this experiment is then  $f_1(N)/f_0(N)$ . As the beam passes through a layer of foil  $dx$ , its change in composition is described by the equations

$$df_1 = (-\sigma_c f_1 + \sigma_l f_0) dx = -df_0. \quad (1)$$

The solution of these equations for constant  $\sigma_c$  and  $\sigma_l$  is

$$\begin{aligned} f_1 &= (\sigma_l/\sigma_c) + [f_1(0) - \sigma_l/\sigma_c] \cdot \exp(-\sigma_c x) \\ f_0 &= (\sigma_c/\sigma_l) + [f_0(0) - \sigma_c/\sigma_l] \cdot \exp(-\sigma_c x) = 1 - f_1, \end{aligned} \quad (2)$$

with

$$\sigma_c \equiv \sigma_l + \sigma_e.$$

The concept of charge equilibrium is applicable if the cross sections change only slightly due to energy change as the beam travels the distance of a mean free path,  $\delta x = \sigma_c^{-1}$ . In this case, once the beam has traveled several mean free paths in the foil, its composition is described almost exactly, in consequence of Eq. (2), by

$$f_1(x)/f_0(x) = \sigma_l(x)/\sigma_c(x). \quad (3)$$

Thus the state of the beam is independent of its initial composition and only changes slowly with the changes in cross sections: a state of near-equilibrium is estab-

<sup>20</sup> S. D. Warsaw, Phys. Rev. **76**, 1759 (1949). Foil thickness in Warsaw's work was obtained by the same method.

TABLE I. Exponents " $n$ " as a function of ion speed. The data are fitted in segments by equations  $R \equiv \sigma_l/\sigma_c = (v/v_1)^n$ . The "light" elements are Be, Al, and Ag.

Elements	Ion energy $E$ , kev	$v/v_0$	$n$	$v_1/v_0$
Light	350	3.75	9.2	2.2
Au			7.0	1.9
Light	300	3.48	8.0	2.0
Au			7.0	1.9
Light	200	2.84	5.8	1.7
Au			4.9	1.6
Light	100	2.01	3.2	1.3
Au			2.6	1.2

lished. As the beam leaves the foil,

$$f_1(N)/f_0(N) = \sigma_l/\sigma_c, \quad (3a)$$

where the cross sections correspond to the energy of the emergent beam. Thus the beam composition gives directly the ratio of loss to capture cross section. Equation (3a) applies to all of the data in this paper.

## VI. RESULTS

All of the results are contained in Fig. 3, which gives the ratios of electron loss to electron capture cross sections for the different ion speeds and media studied. Only one curve is drawn for the elements beryllium and silver, since the data do not reveal any difference in charge state for these media. The aluminum data too are indistinguishable from the solid curve over most of the energy range. However, at the lowest energies studied the beam seemed to be more neutral in aluminum, and these data are represented on a broken line. There is no explanation for this variation in aluminum, and it may not be real. It should be pointed out that experimental error increases at the low energies due to decreased detector sensitivity, but this error still should not exceed about eight percent at the very lowest points.

The gold curve is indistinguishable from the solid line at the lower energies, but for higher energies the beam is more neutral in gold. This is in line with theoretical ideas implying larger capture cross sections in the heavier elements. For the higher energies the gold curve (broken line) is drawn through the most neutral points, since the others are believed to have suffered from a systematic error. This point is discussed under the fourth of the systematic errors considered below.

Current theories generally predict that the capture and loss cross sections will vary with some power of the ion energy. For convenience in the discussion offered below, straight lines have been drawn in Fig. 3 corresponding to the exponents which occur in these theories. As regards the absolute size of the cross sections, these

theories are generally very approximate; therefore the straight lines in Fig. 3 correspond to these theories in exponent only, and their location has no significance.

## VII. SYSTEMATIC ERRORS

While the experiment described here is extremely simple in principle, a number of systematic errors may invalidate the results. Presumably some of these errors are connected with the great inconsistency between the different reports in this field. Therefore several possible errors will be discussed here in some detail.

(1) The beam produces some light by excitation of the residual gas in the vacuum chamber and this light acts like a neutral beam component. While a consideration of the mean free path for excitation indicates that this light should be negligible in amount, the ionic beam has always been quite visible at the end of the accelerator tube, so it was thought best to check this point experimentally. The glass shutter, part  $K$  in Fig. 1, was used for this purpose; with the beam striking the shutter much more light is produced in it than in all of the residual gas. The light produced even with this exaggerated effect was never more than barely detectable with the photo-multiplier.

There remains the possibility that such an effect could occur with ultraviolet light alone. However, at the higher energies the beam from the accelerator was observed to be overwhelmingly charged (as described in the next paragraph), proving that no specious neutral beam was produced. The ultraviolet light effect is not expected to be any stronger at lower ion energies.

(2) The electric field was able to eliminate the charged component of the beam quite completely, and the shield  $L$  prevented detection of any stray radiation produced by this component after it was deflected. This point was confirmed by measuring the composition of a high energy beam with no foil in the beam path; the observed ratio  $f_1/f_0$  was more than two thousand.

(3) It is essential that the beam should not change composition between leaving the foil and entering the deflecting electric field. Such a change may occur from collisions with solid structures such as the collimator walls, or from collisions with the residual gas in the vacuum. The collimation geometry guarantees that there is no error for the first reason: to reach the crystal a particle must pass directly from one collimating hole to the other and can collide with no solid material after leaving the foil. Collisions with the residual gas must be prevented of course by an adequate vacuum. In this experiment the pressure at the vacuum gauge was about  $4 \cdot 10^{-6}$  mm.

Stability of the beam composition was tested by making measurements without the foil in the beam path; such beams should be very predominantly charged. As was pointed out, this was found to be the case for the higher energy beams, but the neutral component became steadily stronger as the energy de-

creased, until at the lowest energies used the ratio  $f_i/f_0$  was only three or four times greater with the foil out than with it in. This effect is much stronger than one would expect from the residual gas with the vacuum stated above. Nevertheless, while the residual gas between magnetic analysis and electric deflection was evidently dense enough to affect the beam strongly at low energies, it still amounted to less than a mean free path for change of charge. Since the distance from foil to electric deflection was only one-seventh of that from magnetic selection to electric deflection, the former is only a very small fraction of a mean free path and the residual gas effect must be negligible.

(4) It is essential that the beam composition should not change at the surface of the foils because of the presence there of oxide layers or films of oil from the diffusion pumps. As to oxide layers, which form on beryllium and aluminum, they are much too thin to change the state of charge, and the results show anyway that the state of charge is probably the same in all elements of atomic numbers between those of beryllium and silver. Deposition of oil is a much more serious problem. All diffusion pumps used were well baffled and equipped with elaborate liquid air traps; nevertheless, oil has sporadically appeared on the targets and foils during experiments in our laboratory. However, in our experience the oil films always build up over a period of hours. Taking advantage of this, we did not expose the vacuum chamber even to liquid-air trapped diffusion pumps, until a few minutes before the start of each run, and then repeated the early points at the end of each run. The consistency of these points proves either that no oil deposited or that the oil layer did not change the beam's state of charge.

The initial and final points in each run were consistent for the three lighter elements studied, but not for gold. In three successive gold runs, the initial points fell on one curve and the later points were displaced toward the curve characteristic of lighter elements. In the last of these runs special care was taken to minimize the oil effect and the displacement of the later points was only slight, so that the data seemed to represent gold legitimately. At any rate there is no question that the beam has a larger neutral component in gold than in the lighter elements, and the oil effect, if significant at all, causes us to underestimate this difference.

It should be noted that oil films on targets and foils can usually be seen, especially after a beam carbonizes them. Visual observation confirms the conclusions stated, in that no oil was observed on the foils after almost all the runs with the three lighter elements. Oil was observed on two of the three thick gold foils.

(5) Another important question is that of the equality of response of the crystal to neutral and to charged particles. The sufficient condition for this equality, in the case of low energy beams, is that charged particles entering the crystal must pick up an electron before traveling an appreciable part of their range.

Because of the large electron capture cross section, this condition is easily satisfied.

(6) Some systematic error is involved in the use of the multiplier gain curve for the higher energy points. Several measurements of this gain curve showed that over the region where the curve was needed (tube voltage varying from 400 to 900 v) the current gain was closely proportional to the eighth power of the tube voltage, with an uncertainty of about one percent in the exponent. For the highest energies studied, where the resulting error is the greatest, this corresponds to a systematic uncertainty of about two percent in the ratio  $\sigma_i/\sigma_e$ .

### VIII. ACCURACY OF THE MEASUREMENTS

The two largest sources of error are the uncertainty in the energy of the beam as it leaves the foil, and the random fluctuations of the beam during the observations.

At the high energy end of the curves in Fig. 3, uncertainties in the measurement of the foil thicknesses and in the available figures for rates of energy loss lead to a probable error of approximately  $\pm 1$  kv in energy of the emergent beam. This is only about one-third of one percent of the beam energy, but appears as an error of about  $\pm 1.5$  percent in the ratio  $\sigma_i/\sigma_e$ , the increase being caused by the steepness of the curve. For the lower energies, at 30 kv, for example, the corresponding numbers are  $\pm 1$  kv or  $\pm 3$  percent in beam energy and  $\pm 2$  percent in  $\sigma_i/\sigma_e$ . Errors in the available data on rates of energy loss displace all the curves taken with a particular element, and errors in the measurement of thickness of a foil displace the curve taken with that foil, but such errors do not produce a random spread from point to point within any run. There is also a permanent uncertainty of about plus or minus one-third of one percent in the beam energy, corresponding to the precision with which the accelerating voltage is known; this last effect may simply translate all of the data *en masse* a small amount to the right or left in a log-log plot like Fig. 3.

Random fluctuations of the beam during the observations produce a spread from point to point. With the very strong collimation used, any slight change in the orientation of the beam, as well as any change in intensity, will strongly affect the current reaching the detector. While the monitoring arrangement described above successfully smooths out fluctuations in intensity, it does not respond well to changes in beam orientation. Judging from the fluctuations observed during runs and from the scatter of the points about a smooth curve, the ratio  $\sigma_i/\sigma_e$  seems to be obtained at each point with a probable error of approximately  $\pm 4$  percent. Since this error is random, the final smooth curve is not so strongly affected, and suffers from an uncertainty roughly between one and two percent because of these fluctuations.

A third significant uncertainty arises from use of the

multiplier tube gain curve, as discussed above. The three types of error compound to a probable error of about three percent over almost the entire range of Fig. 3.

In the case of gold, however, the greatest uncertainty is due to oil films. Because of these films, the ratio  $\sigma_i/\sigma_c$  may appear to be as much as 10 percent greater than its true value in gold.

## IX. INTERPRETATION OF RESULTS

### A. Qualitative Features

The general shape of the curves in Fig. 3 is not unreasonable. At ion speeds of  $v_0$  or greater, the capture and loss cross sections and their ratio are strongly energy-dependent. As the ion speed is brought down to  $v_0$  the cross sections both become large, but cannot much exceed the geometric cross section of the atom. Hence they are no longer as strongly energy dependent and the curve becomes flatter. Unfortunately it was not possible to extend the curves below the energies shown because of insufficient sensitivity. However, the canal-ray data of references 1 through 4, while too inconsistent to permit quantitative analysis, show that as the ion energy decreases still further, the loss cross section rapidly falls off and the beam becomes predominantly neutral.

As the energy increases, the ratio  $\sigma_i/\sigma_c$  is seen to become more and more energy-dependent. This is perhaps to be expected, since classical theory, which applies at lower speeds, predicts that  $\sigma_c$  will vary with the inverse sixth power of the ion velocity, while quantum theory, which is applicable to ions of much higher speed, suggests a twelfth power dependence.

### B. Basis for Comparison with Theory

As will be brought out in the following discussion, the theory of the interaction between the fast ions and the medium is inadequate for the ion energies of the present data. Indeed, present theory is weakest in the interesting region of ion speeds near  $v_0$ . This prevents a really satisfactory study of the data beyond an empirical level. But in order to provide some link with present thought, an analytical procedure has been carried out.

The existing theories each indicate that the ratio of capture and loss cross sections will be proportional to some power of the ion speed. For the sake of comparison with these theories, the data have been analyzed to give values for this power " $n$ " as a function of ion speed. Specifically, tangents were drawn to the log-log curves of Fig. 3 and the tangents were fitted by equations of the form  $R=(v/v_1)^n$ ; the parameters " $n$ " and " $v_1$ " are tabulated in Table I. Experimentation with various ways of drawing the curves and tangents shows that each exponent is defined by the data with a leeway of approximately  $\pm 0.2$ .

Since the slope changes considerably over the entire energy range in Fig. 3, it is clear that the entire curve

cannot be described by a power law. However, where the slope is not rapidly changing, a power law applies fairly well to each limited part of the range, and the tangent in that region reveals its exponent.

### C. Theory of Ionization

So far as ionization of the incident hydrogen beam is concerned, Bohr<sup>15</sup> divides the ionizing media into several classes. The lightest media are such that most orbital electrons remain generally a distance of  $a_0$  or greater from their nuclei. ( $a_0$  is the Bohr radius  $\hbar^2/me^2$ .) For such media, collisions with the incident system will either be so distant that the ionizing field is almost entirely screened and the ionizing effect is negligible, or else the incident electron will come close to some one particle in the medium, nucleus or electron, and will undergo a collision in which all other particles may be neglected. Thus for sufficiently light media one may simply sum over the ionizing effects of all particles in the medium, attributing a Coulomb field to each. In this case Bohr estimates a total ionization cross section

$$\sigma_i = 4\pi a_0^2 (Z^2 + Z) (v_0/v)^2, \quad (4)$$

where  $Z$  is the atomic number of the stopping material. The term in  $Z^2$  corresponds to ionization by the nucleus and that in  $Z$  to a sum over all the orbital electrons in each atom.

For somewhat heavier media the inner electrons are closer to the nuclei and the incident system encounters not separate Coulomb fields, but the screened fields of the nuclei. The situation is much more complicated and requires further analysis. Bohr defines the parameter  $\zeta$  as an index of the degree of screening of the nuclear field:  $\zeta \equiv b/a$ , where  $b$  is the distance of closest approach to the unscreened nucleus, and  $a$  is the length characterizing the exponential decrease of the screened field. In the case of ionization of the hydrogen atom by the nuclear fields in the medium,  $\zeta \cong 2Z^{4/3} (v_0/v)^2$ . Bohr then shows that so long as  $\zeta$  is approximately unity, the most important collisions occur in a region where the medium potential varies as  $r^{-2}$ , and furthermore that ionization occurs here only if the incident electron is deflected so strongly that classical mechanics may be correctly applied. On this basis he estimates the cross section  $\sigma_i$  to be

$$\sigma_i \sim \pi a_0^2 Z^{\frac{1}{3}} (v_0/v). \quad (5)$$

For the velocity range of this experiment,  $\zeta$  is near one for a very limited range of elements from lithium through carbon, roughly speaking. Thus for aluminum and heavier elements, we are already dealing with cases of much stronger screening and different approximations are needed. As a matter of fact, neither classical mechanics nor the Born approximation can properly be applied in these cases, but it will be worth while to note the conclusions suggested by each of these approximations.

In the classical picture, for larger  $Z$  and stronger

screening, the distance of closest approach is only slightly increased, but the field inside  $r=a$  becomes so strong that incident electrons moving towards this region are almost certainly ionized. The cross section  $\sigma_l$  therefore comes to depend on  $v$  even less strongly than the first power, and remains of the order  $\sigma_l \sim \pi a^2$ .\*

According to the Born approximation, for very strong screening the scattering of the incident electron by the nuclear field approaches spherical symmetry in the center-of-mass system, and the total scattering cross section becomes independent of the relative velocities.† The ionization cross section will then depend, roughly speaking, only on the size of the critical angle at which energy transfer is great enough to free the electron. This again implies a very weak dependence on velocity, weaker than the first power. The analysis is not really applicable because, for the present data, the incident waves are strongly perturbed by the collision, which invalidates the Born approximation.

However, both classical and simple quantum-mechanical analysis imply that  $\sigma_l$  becomes less dependent on velocity as  $Z$  increases. Furthermore, with still larger values of  $Z$  and very strong screening, the field is so strong within a region of radius approximately  $a_0$  that ionization must occur, and the cross section is then almost independent of velocity.

To summarize, we may expect the following behavior of the cross section for ionization of hydrogen atoms in the beam:

For very light media, up to beryllium:

$$\sigma_l \sim 4\pi a_0^2 (Z^2 + Z) (v_0/v)^2. \quad (4)$$

From beryllium, through carbon:

$$\sigma_l \sim \pi a_0^2 Z^4 (v_0/v). \quad (5)$$

From carbon on: the dependence on  $v$  should be weaker than the first power. It should be progressively weaker in aluminum, silver, and gold, and almost non-existent in gold.

The equations above become completely inapplicable below some ion speed of the order of  $v_0$ , since  $\sigma_l$  then decreases as  $v$  decreases. This speed should coincide roughly with the maxima in the proton stopping curves, which occur near  $v = 2v_0$ .

The equations above are consistent with some previous experiments. Jacobsen's experiments on fast alpha-particles in hydrogen agree with Eq. (4), and Rutherford's data on fast alpha-particles in air with Eq. (5). In Rutherford's work the parameter  $\zeta$  is nearly unity, so that Eq. (5) properly applies.

Earlier work also shows how well these ideas may be applied to ion speeds as low as  $2v_0$  to  $4v_0$ . No direct measurements of  $\sigma_l$  are available in this velocity range. However, data on the energy loss of ions also provide information about ionization; as Fano has shown, this

TABLE II. Exponents for the velocity dependence of  $R \equiv \sigma_l/\sigma_e$ ,  $\sigma_l$ , and  $\sigma_e$ .

Element	$n_R$ (observed)	$n_l$ (estimated)	$n_e$ ( $n_l - n_R$ )
Be	9.2	-1.5	-11
Al	9.2	-0.5	-10
Ag	9.2	0	-9
Au	7.0	0	-7

energy loss is proportional to the ionization of the stopping medium.<sup>21</sup> On this basis, Warshaw's stopping data indicate that the power law most suitable for the ionization of the medium is between  $v^{-0.5}$  and  $v^{-1}$  for  $2v_0 < v < 4v_0$ , while Bohr's analyses lead to a form  $v^{-1}$ .

It may be concluded reliably then that in the present experiments the velocity dependence of the ionization cross section varies between  $v^{-2}$  and  $v^0$ , in a manner which is fairly well understood. At any rate, the suitable exponent should never be unknown to an extent greater than  $\pm 0.5$ . On the other hand, the capture cross section depends very strongly on  $v$  and there is no complete theory for it. The present data will therefore be considered chiefly as descriptive of the capture cross section.

#### D. Theory of Capture

To provide some theoretical basis for considering the velocity dependence of  $\sigma_e$ , Bohr divides stopping media into two classes. In the first, none of the electrons in the medium have speeds as great as  $v$ . Capture must then occur by a double process; first an electron gains energy from the incident particle and then, in a second collision with its own nucleus, it is set into a direction which makes capture possible. For such a process the classical calculation by Thomas indicates a probability varying as  $v^{-5.5}$ ; the classical theory, however, does not apply to ions as fast as  $v_0$  or faster. The corresponding quantum theory calculation, while it cannot be described by means of the orbital picture, also reveals the process to be very strongly velocity dependent; the calculation of Brinkman and Kramers<sup>13</sup> indicates a dependence on  $v^{-12}$ . The quantum-mechanical calculation also cannot be expected to apply well to the present data, since it is based on the Born approximation and assumes that  $v \gg v_0$ .

For heavier media, however, Bohr proposes a very different mechanism of capture; since some of the electrons in the medium already have a speed as large as  $v$ , these may be given the same speed and direction as the incident ion, and then captured, as a result of just one collision. A statistical estimate of such collisions leads Bohr† to the equation

$$\sigma_e \sim 4\pi a_0^2 Z^{\frac{1}{2}} (v_0/v)^6 \quad (6)$$

for such cases.

These estimates may now be compared with the present data. Table I shows the observed behavior of the

\* See reference 15, p. 31.

† See reference 15, Eq. (1.4.5).

<sup>21</sup> U. Fano, Phys. Rev. **70**, 44 (1946).

‡ See reference 15, Eq. (4.3.5).



ratio  $\sigma_i/\sigma_c$ . From the previous discussion we may assign reasonable exponents, for the behavior of  $\sigma_i$  alone. Combining the two sets of exponents, one finds the behavior of  $\sigma_c$  alone. This procedure is carried out in Table II, for the ions with an energy of 350 kv.

Thus the capture cross section is more dependent on velocity than is suggested by the process Bohr proposes, in which capture is a single collision process involving electrons of orbital speeds near  $v$ . As the ion speed increases, the velocity dependence continues to become stronger for the lighter media, suggesting an approach to the quantum-mechanical approximation of Brinkman and Kramers. However, the dependence on velocity becomes progressively less as  $Z$  increases, and in the case of gold it is almost as predicted by Bohr's one-collision process.

### E. Dependence of the Charge State on the Medium

One of the most remarkable features of the data is that the composition of the beam is found to be almost the same, for all speeds studied, in the media beryllium, silver, gold, and aluminum. This indifference of the beam composition to the medium has been noted previously by the experimenters referred to: Henderson,<sup>7</sup> Briggs,<sup>8</sup> and Gerthsen<sup>9</sup> could find no difference between the charge composition of alpha-ray beams in aluminum, mica, copper, silver, and gold, and Kapitza<sup>6</sup> even found the same charge composition in air and in hydrogen for alphas of speeds between  $2v_0$  and  $3v_0$ . Rutherford reported that alpha-beams were very slightly more neutral in gold than in mica, and Jacobsen observed that quite fast alphas (speed around  $8v_0$ ) are definitely less neutralized in hydrogen than in air. In the hydrogen canal-ray experiments, observers have reported different charge compositions in oxygen, nitrogen, and air, but inconsistencies in these data show that these results may be due to experimental errors. The over-all evidence is that the charge composition is independent of the medium over a wide range of values of  $Z$ , from beryllium through silver at least, and remains almost the same in gold.

Theoretically it is expected that  $\sigma_i$  and  $\sigma_c$  will both be almost independent of  $Z$  for the heavier elements. However, there is no explanation at present for the uniformity of beam composition from beryllium through silver.

### F. Ion Speed for Which $\sigma_i = \sigma_c$

For calculations of the stopping of fission fragments, it is important to know the ion speed for which  $\sigma_i = \sigma_c$ . The data were carried down through this point in the case of aluminum, and the speed is found to be  $0.95 \pm 0.05v_0$ . This speed is somewhat lower than the value of  $1.1v_0$  given by Bartels for canal rays in air. The fact is once again confirmed that capture and loss probabilities are about equal for ionic orbits of speeds near the speed of the ion.

### X. CONCLUSIONS

The ratio of the loss to the capture cross section for proton beams of speeds  $v_0$  to  $4v_0$  in various metals behaves qualitatively as one might expect from present theory. Quantitatively, in beryllium, aluminum, and silver, the capture cross section depends on the velocity more strongly than one would expect on the assumption that capture is mainly of electrons with speed near  $v$ . In beryllium, this dependence becomes greater as the ion speed increases, and at an ion speed of  $4v_0$  it is almost as great as that predicted by the quantum-mechanical theory of Brinkman and Kramers. However, in gold the velocity dependence of the capture cross section is almost as predicted on the assumption that the captured electrons have speeds near  $v$  (Bohr's crude statistical model).

For the four media studied, the beam composition is almost identical, being indistinguishable in the three lighter media and slightly more neutral in gold at ion speeds greater than two  $v_0$ . Existing theory offers no explanation for this lack of dependence on medium.

The capture and loss cross sections are observed to be equal for hydrogen ions of speed  $v = 0.95v_0$ .

The ratio  $\sigma_i/\sigma_c$  is also useful for corrections to the stopping theory for light nuclei. For this purpose it is convenient to note these approximate values for hydrogen beams in metals:  $\sigma_i/\sigma_c = 10$  at  $v = 2.5v_0$  and  $\sigma_i/\sigma_c = 100$  at  $v = 3.2v_0$ .

I wish to thank S. K. Allison for proposing this work and for his help during its progress, A. J. Dempster for suggestions in connection with the design of the vacuum chamber, S. D. Warshaw for his very close collaboration in the design and initial testing of the apparatus, and David Bushnell for sharing the work in constructing parts and taking the measurements.